The Star Formation Newsletter

A community newsletter on Star and Planet Formation research

No. 350 — 27 February 2022

Editor: João Alves www.starformation.news

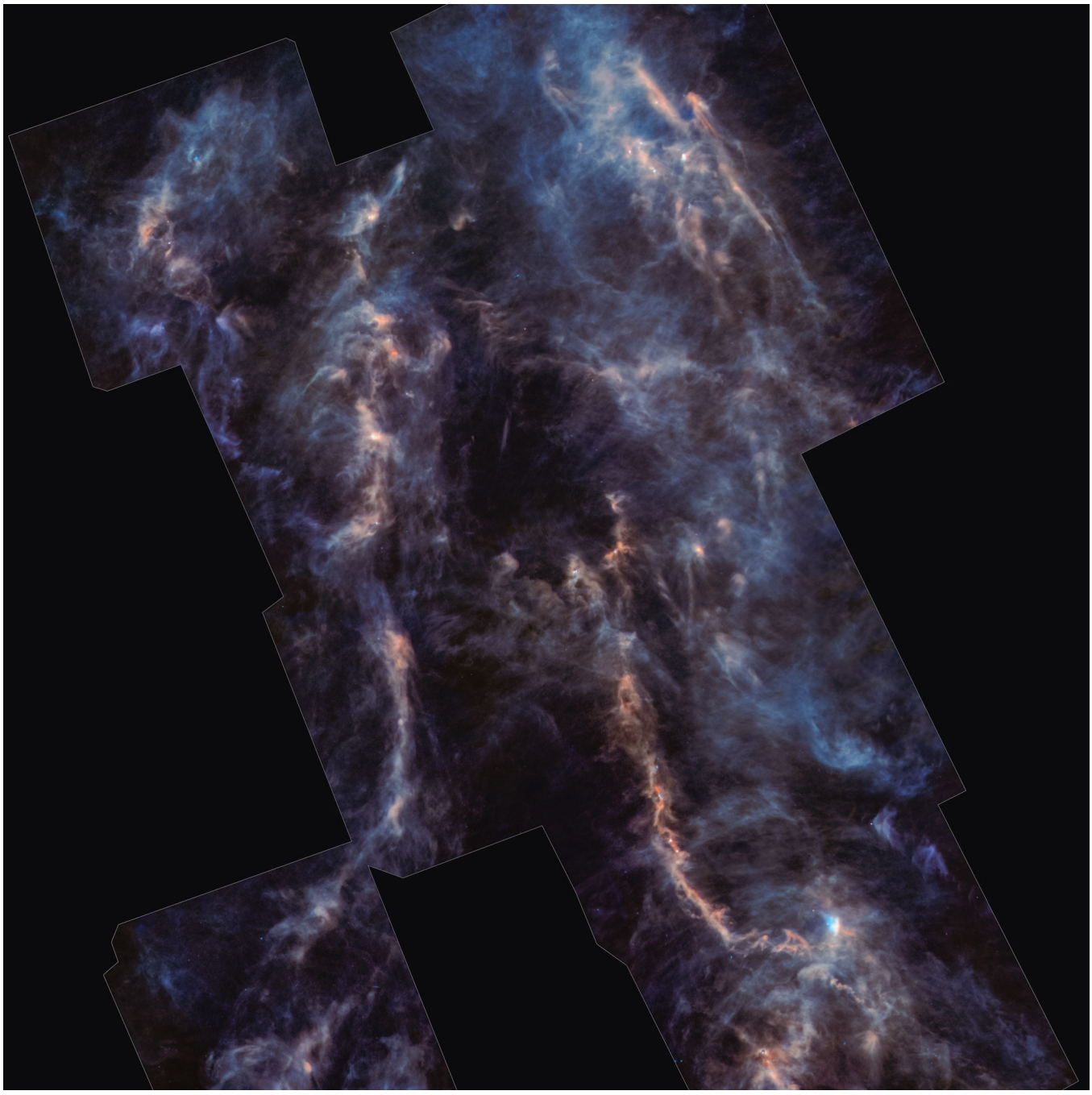

Links to sections

Interviews	Reviews	Perspective	Favorite objects	Archive
Meetings	Jobs	New PhDs	Announcements	Books

Cover image caption

The Taurus Molecular Cloud as seen by ESA's Herschel observatory. Together with Ophiuchus, these are the closest molecular cloud complexes to Earth (distance 140 pc), found at the opposite sides of the Local Bubble. The resolution of the image is around 5000 au. The red hue represents denser, colder gas (T ∼10 K), while the blue hue represents more diffuse, warmer gas (T ∼15 K). Many benchmark objects in (low-mass) star formation, like young stellar objects, circumstellar disks, jets, outflows, as well as filaments and dense cores, are part of this region. This four-color image combines Herschel observations at 160 microns (blue), 250 microns (green), 350 microns (split between green and red), and 500 microns (red). Credit: ESA/Herschel. Color composite by R. Hurt.

Note from the Editor

The Star Formation Newsletter is now on the web at **www.starformation.news**. This PDF file contains the monthly Abstracts and links to the different Newsletter sections. Red text in this PDF is a url link. Submitting an abstract to the SFN is as simple as entering the arXiv ID (e.g., 2006.10139) in a web form on the SFN web site. **Do not remove the LaTeX formatting when submitting to the arXiv**. If you do, your abstract will not look great either at the arXiv or the SFN.

Abstracts

1. The sharp ALMA view of infall and outflow in the massive protocluster G31.41+0.31

M. T. Beltrán, V. M. Rivilla, R. Cesaroni, D. Galli, L. Moscadelli, A. Ahmadi, H. Beuther, S. Etoka, C. Goddi, P. D. Klaassen, R. Kuiper, M. S. N. Kumar, A. Lorenzani, T. Peters, Á. Sánchez-Monge, P. Schilke, F. van der Tak, S. Vig ★ Context. To better understand the formation of high-mass stars, it is fundamental to investigate how matter accretes onto young massive stars, how it is ejected, and how all this differs from the low-mass case. The massive protocluster G31.41+0.31 is the ideal target to study all these processes because observations at millimeter and centimeter wavelengths have resolved the emission of the Main core into at least four massive dust continuum sources, named A, B, C, and D, within 1" or 0.018 pc, and have identified signatures of infall and several outflows associated with the core. Aims. We study the interplay between infall and outflow in G31.41+0.31 by investigating at a spatial resolution of a few 100 au their properties and their possible impact on the core. Methods. We carried out molecular line observations of typical high-density tracers, such as CH3CN or H2CO, and shock and outflow tracers, such as SiO, with ALMA at 1.4 mm that achieved an angular resolution of 0.09" (340 au). Results. The observations have revealed inverse P-Cygni profiles in CH3CN and H2CO toward the four sources embedded in the Main core, suggesting that all of them are undergoing collapse. The infall rates, estimated from the red-shifted absorption are on the order of 1E-2 Msun/yr. The individual infall rates imply that the accretion timescale of the Main core is an order of magnitude smaller than its rotation timescale. This confirms that rotating toroids such as the G31 Main core are non-equilibrium, transient collapsing structures that need to be constantly replenished with fresh material from a large-scale reservoir. For sources B, C, and D, the infall could be accelerating inside the sources, while for source A, the presence of a second emission component complicates the interpretation.

2. Gravity or turbulence V: Star forming regions undergoing violent relaxation

Andrea Bonilla-Barroso, J. Ballesteros-Paredes, Jesus Hernández, Luis Aguilar, Manuel Zamora, Lee W. Hartmann, Aleksandra Kuznetsova, Vianey Camacho, Verónica Lora ★ Using numerical simulations of the formation and

evolution of stellar clusters within molecular clouds, we show that the stars in clusters formed within collapsing molecular cloud clumps exhibit a constant velocity dispersion regardless of their mass, as expected in a violent relaxation processes. In contrast, clusters formed in turbulence-dominated environments exhibit an *inverse* mass segregated velocity dispersion, where massive stars exhibit larger velocity dispersions than low-mass cores, consistent with massive stars formed in massive clumps, which in turn, are formed through strong shocks. We furthermore use Gaia EDR3 to show that the stars in the Orion Nebula Cluster exhibit a constant velocity dispersion as a function of mass, suggesting that it has been formed by collapse within one free-fall time of its parental cloud, rather than in a turbulence-dominated environment during many free-fall times of a supported cloud. Additionally, we have addressed several of the criticisms of models of collapsing star forming regions: namely, the age spread of the ONC, the comparison of the ages of the stars to the free-fall time of the gas that formed it, the star formation efficiency, and the mass densities of clouds vs the mass densities of stellar clusters, showing that observational and numerical data are consistent with clusters forming in clouds undergoing a process of global, hierarchical and chaotic collapse, rather than been supported by turbulence.

3. Scanning disk rings and winds in CO at 0.01-10 au: a high-resolution M-band spectroscopy survey with IRTF-iSHELL

Andrea Banzatti, Kirsten M. Abernathy, Sean Brittain, Arthur D. Bosman, Klaus M. Pontoppidan, Adwin Boogert, Stanley Jensen, John Carr, Joan Najita, Sierra Grant, Rocio M. Sigler, Michael A. Sanchez, Joshua Kern, John T. Rayner ★ We present an overview and first results from a M-band spectroscopic survey of planet-forming disks performed with iSHELL on IRTF, using two slits that provide resolving power R ≈ 60,000-92,000 (5-3.3 km/s). iSHELL provides a nearly complete coverage at 4.52-5.24 μm in one shot, covering > 50 lines from the R and P branches of ^{12}CO and ^{13}CO for each of multiple vibrational levels, and providing unprecedented information on the excitation of multiple emission and absorption components. Some of the most notable new findings of this survey are: 1) the detection of two CO Keplerian rings at < 2 au (in HD 259431), 2) the detection of H_2O ro-vibrational lines at 5 μm (in AS 205 N), and 3) the common kinematic variability of CO lines over timescales of 1-14 years. By homogeneously analyzing this survey together with a previous VLT-CRIRES survey of cooler stars, we discuss a unified view of CO spectra where emission and absorption components scan the disk surface across radii from a dust-free region within dust sublimation out to ≈ 10 au. We classify two fundamental types of CO line shapes interpreted as emission from Keplerian rings (double-peak lines) and a disk surface plus a low-velocity part of a wind (triangular lines), where CO excitation reflects different emitting regions (and their gas-to-dust ratio) rather than just the irradiation spectrum. A disk+wind interpretation for the triangular lines naturally explains several properties observed in CO spectra, including the line blue-shifts, line shapes that turn into narrow absorption at high inclinations, and the frequency of disk winds as a function of stellar type.

4. CH_3CN deuteration in the SVS13-A Class I hot-corino. SOLIS XV

Eleonora Bianchi, Cecilia Ceccarelli, Claudio Codella, Ana López-Sepulcre, Satoshi Yamamoto, Nadia Balucani, Paola Caselli, Linda Podio, Roberto Neri, Rafael Bachiller, Cécile Favre, Francesco Fontani, Bertrand Lefloch, Nami Sakai, Dominique Segura-Cox ★ We studied the line emission from CH3CN and its deuterated isotopologue CH_2DCN towards the prototypical Class I object SVS13-A, where the deuteration of a large number of species has already been reported. Our goal is to measure the CH_3CN deuteration in a Class I protostar, for the first time, in order to constrain the CH_3CN formation pathways and the chemical evolution from the early prestellar core and Class 0 to the evolved Class I stages. We imaged CH2DCN towards SVS13-A using the IRAM NOEMA interferometer at 3mm in the context of the Large Program SOLIS (with a spatial resolution of 1.8"x1.2"). The NOEMA images have been complemented by the CH_3CN and CH_2DCN spectra collected by the IRAM-30m Large Program ASAI, that provided an unbiased spectral survey at 3mm, 2mm, and 1.3mm. The observed line emission has been analysed using LTE and non-LTE LVG approaches. The NOEMA/SOLIS images of CH2DCN show that this species emits in an unresolved area centered towards the SVS13-A continuum emission peak, suggesting that methyl cyanide and its isotopologues are associated with the hot corino of SVS13-A, previously imaged via other iCOMs. In addition, we detected 41 and 11 ASAI transitions of CH_3CN and CH2DCN, respectively, which cover upper level energies (Eup) from 13 to 442 K and from 18 K to 200 K, respectively. The derived [CH2DCN]/[CH3CN] ratio is ∼9%. This value is consistent with those measured towards prestellar cores and a factor 2-3 higher than those measured in Class 0 protostars. Contrarily to what expected for other molecular species, the CH3CN deuteration does not show a decrease in SVS13-A with respect to measurements in younger prestellar cores and Class 0 protostars. Finally, we discuss why our new results suggest that CH3CN was likely synthesised via gas-phase reactions and frozen onto the dust grain mantles during the cold prestellar phase.

5. Deuterium fractionation as a multi-phase component tracer in the Galactic Centre

L. Colzi, J. Martín-Pintado, V. M. Rivilla, I. Jiménez-Serra, S. Zeng, L. F. Rodríguez-Almeida, F. Rico-Villas, S. Martín, M. A. Requena-Torres ★ The Central Molecular Zone (CMZ) contains most of the mass of our Galaxy but its star formation rate is one order of magnitude lower than in the Galactic disc. This is likely related to the fact that the bulk of the gas in the CMZ is in a warm (>100 K) and turbulent phase with little material in the pre-stellar phase. We present in

this Letter observations of deuterium fractionation (D/H ratios) of HCN, HNC, HCO^+, and N_2H^+ towards the CMZ molecular cloud G+0.693-0.027. These observations clearly show, for the first time, the presence of a colder, denser, and less turbulent narrow component, with a line width of ∼9 km s^{-1}, in addition to the warm, less dense and turbulent broad component with a line width of ∼20 km s^{-1}. The very low D/H ratio $\leq 6\times10^{-5}$ for HCO^+ and N_2H^+, close to the cosmic value ($\sim 2.5\times10^{-5}$), and the high D/H ratios $>4\times10^{-4}$ for HCN and HNC derived for the broad component, confirm the presence of high-temperatures deuteration routes for nitriles. For the narrow component we have derived D/H ratios $>10^{-4}$ and excitation temperatures of 7 K for all molecules, suggesting kinetic temperatures ≤30 K and H_2 densities $\geq 5\times10^4$ cm^{-3}, at least one order of magnitude larger than for the broad component. The method presented in this Letter allows to identify clouds on the verge of star formation, i.e. under pre-stellar conditions, towards the CMZ. This method can also be used for the identification of such clouds in external galaxies.

6. Completing the Protostellar Luminosity Function in Cygnus-X with SOFIA/FORCAST Imaging

Yingjie Cheng, Robert A. Gutermuth, Stella Offner, Mark Hemeon-Heyer, Hans Zinnecker, S. Thomas Megeath, Riwaj Pokhrel ★ We present a new SOFIA/FORCAST mid-IR survey of luminous protostars and crowded star-forming environments in Cygnus X, the nearest million-solar mass molecular cloud complex. We derive bolometric luminosities for over 1000 sources in the region with these new data in combination with extant Spitzer and UKIDSS photometry, with 63 new luminous protostar candidates identified by way of the high quality SOFIA/FORCAST data. By including FORCAST data, we construct protostellar luminosity functions (PLFs) with improved completeness at the high luminosity end. The PLFs are well described by a power law function with an index of -0.5. Based on the Herschel temperature and column density measurements, we find no obvious dependence of the PLFs on the local gas temperature, but PLFs in regions of high stellar density or gas column density exhibit some excess at higher luminosities. Through the comparison between our observed PLFs and existing accretion models, both the turbulent core (TC) and the competitive accretion (CA) models are consistent with our results, while the isothermal sphere (IS) model is disfavored. The implications of these results on the star formation process are discussed.

7. ALMA's view of the M-dwarf GSC 07396-00759's edge-on debris disc: AU Mic's coeval twin

Patrick F. Cronin-Coltsmann, Grant M. Kennedy, Christian Adam, Quentin Kral, Jean-François Lestrade, Sebastian Marino, Luca Matrà, Simon J. Murphy, Johan Olofsson, Mark C. Wyatt ★ We present new ALMA Band 7 observations of the edge-on debris disc around the M1V star GSC 07396-00759. At 20 Myr old and in the beta Pictoris Moving Group along with AU Mic, GSC 07396-00759 joins it in the handful of low mass M-dwarf discs to be resolved in the sub-mm. With previous VLT/SPHERE scattered light observations we present a multi-wavelength view of the dust distribution within the system under the effects of stellar wind forces. We find the mm dust grains to be well described by a Gaussian torus at 70 au with a FWHM of 48 au and we do not detect the presence of CO in the system. Our ALMA model radius is significantly smaller than the radius derived from polarimetric scattered light observations, implying complex behaviour in the scattering phase function. The brightness asymmetry in the disc observed in scattered light is not recovered in the ALMA observations, implying that the physical mechanism only affects smaller grain sizes. High resolution follow-up observations of the system would allow investigation into its unique dust features as well as provide a true coeval comparison for its smaller sibling AU Mic, singularly well observed amongst M-dwarfs systems.

8. Scattering and sublimation: a multi-scale view of μm-sized dust in the inclined disc of HD 145718

Claire L. Davies, Evan A. Rich, Tim J. Harries, John D. Monnier, Anna S. E. Laws, Sean M. Andrews, Jaehan Bae, David J. Wilner, Narsireddy Anugu, Jacob Ennis, Tyler Gardner, Stefan Kraus, Aaron Labdon, Jean-Baptiste le Bouquin, Cyprien Lanthermann, Gail H. Schaefer, Benjamin R. Setterholm, Theo ten Brummelaar ★ We present multi-instrument observations of the disc around the Herbig Ae star, HD 145718, employing geometric and Monte Carlo radiative transfer models to explore the disc orientation, the vertical and radial extent of the near infrared (NIR) scattering surface, and the properties of the dust in the disc surface and sublimation rim. The disc appears inclined at $67-71^\circ$, with position angle, PA $= -1.0-0.6^\circ$, consistent with previous estimates. The NIR scattering surface extends out to ∼ 75 au and we infer an aspect ratio, $h_{\rm scat}(r)/r \sim 0.24$ in J-band; ∼ 0.22 in H-band. Our GPI images and VLTI+CHARA NIR interferometry suggest that the disc surface layers are populated by grains $\gtrsim \lambda/2\pi$ in size, indicating these grains are aerodynamically supported against settling and/or the density of smaller grains is relatively low. We demonstrate that our geometric analysis provides a reasonable assessment of the height of the NIR scattering surface at the outer edge of the disc and, if the inclination can be independently constrained, has the potential to probe the flaring exponent of the scattering surface in similarly inclined ($i \gtrsim 70^\circ$) discs. In re-evaluating HD 145718's stellar properties, we found that the object's dimming events - previously characterised as UX Or and dipper variability - are consistent with dust occultation by grains larger, on average, than found in the ISM. This occulting dust likely originates close to the inferred dust sublimation radius at 0.17 au.

9. Do the majority of stars form as gravitationally unbound?

František Dinnbier, Pavel Kroupa, Richard I. Anderson ★ Some of the youngest stars (age $\lesssim$ 10 Myr) are clustered, while many others are observed scattered throughout star forming regions or in complete isolation. It has been intensively debated whether the scattered or isolated stars originate in star clusters, or if they form truly isolated, which could help constrain the possibilities how massive stars are formed. We adopt the assumption that all stars form in gravitationally bound star clusters embedded in molecular cloud cores (Γ-1 model), which expel their natal gas, and compare the fraction of stars found in clusters with observational data. The star clusters are modelled by the code nbody6, which includes stellar and circumbinary evolution, gas expulsion, and the external gravitational field of their host galaxy. We find that small changes in the assumptions in the current theoretical model estimating the fraction, Γ, of stars forming in embedded clusters have a large influence on the results, and we present a counterexample as an illustration. This calls into question theoretical arguments about Γ in embedded clusters, and it suggests that there is no firm theoretical ground for low Γ in galaxies with lower star formation rates (SFRs). Instead, the assumption that all stars form in embedded clusters is in agreement with observational data for the youngest stars (age $\lesssim$ 10 Myr). In the Γ-1 scenario, the observed fraction of the youngest stars in clusters increases with the SFR only weakly; the increase is caused by the presence of more massive clusters in galaxies with higher SFRs, which release fewer stars to the field in proportion to their mass. The Γ-1 model yields a higher fraction of stars in clusters for older stars (age between 10 and 300 Myr) than what is observed. This discrepancy can be caused by interactions with molecular clouds.

10. Successive deuteration in low-mass star-forming regions: the case of D_2-methanol (CHD_2OH) in IRAS 16293-2422

Maria N. Drozdovskaya, Laurent H. Coudert, Laurent Margulès, Audrey Coutens, Jes K. Jørgensen, Sébastien Manigand ★ Accurate quantification of the column density of di-deuterated methanol is a key missing puzzle piece in the otherwise thoroughly constrained family of D-bearing methanol in the deeply embedded low-mass protostellar system and astrochemical template source IRAS16293-2422. A spectroscopic dataset for astrophysical purposes is built for CHD_2OH and made publicly available to facilitate accurate characterization of this species in astrochemical surveys. The newly computed line list and partition function are used to search for CHD_2OH towards IRAS16293-2422 A and B in data from ALMA-PILS. Only non-blended, optically thin lines of CHD_2OH are used for the synthetic spectral fitting. The constructed spectroscopic database contains line frequencies and strengths for 7417 transitions in the 0 to 500 GHz frequency range. ALMA-PILS observations in the 329-363 GHz range are used to identify 105 unique, non-blended, optically thin line frequencies of CHD_2OH for synthetic spectral fitting. The derived excitation temperatures and column densities yield high D/H ratios of CHD_2OH in IRAS 16293-2422 A and B of 7.5±1.1not higher than in other low-mass star-forming regions. Di-deuterated molecules consistently have higher D/H ratios than their monodeuterated counterparts in all low-mass protostars, which may be a natural consequence of H-D substitution reactions as seen in laboratory experiments. The Solar System's natal cloud, as traced by comet 67P/Churyumov-Gerasimenko, may have had a lower initial abundance of D, been warmer than the cloud of IRAS16293-2422, or been partially reprocessed. In combination with accurate spectroscopy, a careful spectral analysis, and a consideration of the underlying assumptions, successive deuteration is a robust window on the physicochemical provenance of star-forming systems.

11. The impact of cosmic-ray attenuation on the carbon cycle emission in molecular clouds

Brandt A. L. Gaches, Thomas G. Bisbas, Shmuel Bialy ★ Observations of the emission of the carbon cycle species (C, C+ CO) are commonly used to diagnose gas properties in the interstellar medium but are significantly sensitive to the cosmic-ray ionization rate. The carbon-cycle chemistry is known to be quite sensitive to the cosmic-ray ionization rate, ζ, controlled by the flux of low-energy cosmic rays which get attenuated through molecular clouds. However, astrochemical models commonly assume a constant cosmic-ray ionization rate in the clouds. We investigate the effect of cosmic-ray attenuation on the emission of carbon cycle species from molecular clouds, in particular the [CII] 158 μm, [CI] 609 μm and CO (J = 1 - 0) 115.27 GHz lines. We use a post-processed chemical model of diffuse and dense simulated molecular clouds and quantify the variation in both column densities and velocity integrated line emission of the carbon cycle with different cosmic-ray ionization rate models. We find that the abundances and column densities of carbon cycle species is significantly impacted by the chosen cosmic-ray ionization rate model: no single constant ionization rate can reproduce the abundances modelled with an attenuated cosmic-ray model. Further, we show that constant ionization rate models fail to simultaneously reproduce the integrated emission of the lines we consider, and their deviations from a physically derived cosmic-ray attenuation model is too complex to be simply corrected. We demonstrate that the two clouds we model exhibit a similar average $A_{\rm V,eff} - n_{\rm H}$ relationship, resulting in an average relation between the cosmic-ray ionization rate and density $\zeta(n_{\rm H})$. We conclude by providing a number of implementation recommendations for CRs in astrochemical models, but emphasize the necessity for column-dependent cosmic-ray ionization rate prescriptions.

12. Importance of source structure on complex organics emission. I. Observations of CH_3OH from low-mass to high-mass protostars

M. L. van Gelder, P. Nazari, B. Tabone, A. Ahmadi, E. F. van Dishoeck, M. T. Beltrán, G. A. Fuller, N. Sakai, Á. Sánchez-Monge, P. Schilke, Y. -L. Yang, Y. Zhang ★ Complex organic molecules (COMs) are often observed toward embedded Class 0 and I protostars. However, not all Class 0 and I protostars exhibit COMs emission. In this work, variations in methanol (CH_3OH) emission are studied to test if absence of CH_3OH emission can be linked to source properties. Combining both new and archival observations with ALMA and sources from the literature, a sample of 184 low-mass and high-mass protostars is investigated. The warm ($T > 100$ K) gaseous CH_3OH mass, M_{CH_3OH}, is determined for each source using primarily optically thin isotopologues. On average, Class I protostellar systems seem to have less warm M_{CH_3OH} ($< 10^{-10}$ $M_\odot$) than younger Class 0 sources ($\sim 10^{-7}$ $M_\odot$). High-mass sources in our sample show higher warm M_{CH_3OH} up to $10^{-7} - 10^{-3}$ $M_\odot$. To take into account the effect of the source's overall mass on M_{CH_3OH}, a normalized CH_3OH mass is defined as $M_{CH_3OH}/M_{dust,0}$, where $M_{dust,0}$ is the cold + warm dust mass within a fixed radius. Excluding upper limits, a simple power-law fit to the normalized warm CH_3OH masses results in $M_{CH_3OH}/M_{dust,0} \propto L_{bol}^{0.71\pm0.05}$. This is in good agreement with a simple hot core toy model which predicts that the normalized M_{CH_3OH} increases with $L_{bol}^{0.75}$ due to the snowline moving outward. Sources for which the size of the disk is equivalent or smaller than the estimated 100 K radius agree well with the best-fit power-law model, whereas sources with significantly larger disks show up to two orders of magnitude lower normalized warm CH_3OH masses. Based on the latter results, we suggest that source structure such as a disk can result in colder gas and thus fewer COMs in the gas phase. Additionally, optically thick dust can hide the emission of COMs.

13. A new planet candidate detected in a dust gap of the disc around HD 163296 through localised kinematic signatures. An observational validation of the Discminer

Andres F. Izquierdo, Stefano Facchini, Giovanni P. Rosotti, Ewine F. van Dishoeck, Leonardo Testi ★ We report the robust detection of coherent, localised deviations from Keplerian rotation possibly associated with the presence of two giant planets embedded in the disc around HD 163296. The analysis is performed using the DISCMINER channel-map modelling framework on ^{12}CO $J = 2 - 1$ DSHARP data. Not only orbital radius, but also azimuth of the planets are retrieved by our technique. One of the candidate planets, detected at $R = 94 \pm 6$ au, $\phi = 50 \pm 3°$ (P94), is near the centre of one of the gaps in dust continuum emission, and is consistent with a planet mass of 1 M_{Jup}. The other planet, located at $R = 261 \pm 4$ au, $\phi = 57 \pm 1°$ (P261), is in the region where a velocity kink was previously observed in ^{12}CO channel maps. Also, we provide a simultaneous description of the height and temperature of the upper and lower emitting surfaces of the disc, and propose the line width as a solid observable to track gas substructure. Using azimuthally averaged line width profiles we detect gas gaps at $R = 38$ au, $R = 88$ au, and $R = 136$ au, closely matching the location of their dust and kinematical counterparts. Furthermore, we observe strong azimuthal asymmetries in line widths around the gas gap at $R = 88$ au, possibly linked to turbulent motions driven by the P94 planet. Our results confirm that the DISCMINER is capable of finding localised, otherwise unseen velocity perturbations thanks to its robust statistical framework, but also that it is well suited for studies of the gas properties and vertical structure of protoplanetary discs.

14. A population of transition disks around evolved stars: Fingerprints of planets? Catalog of disks surrounding Galactic post-AGB binaries

Jacques Kluska, Hans Van Winckel, Quentin Coppée, Glenn-Michael Oomen, Devika Kamath, Valentin Bujarrabal, Michiel Min ★ Post-asymptotic giant branch (post-AGB) binaries are surrounded by massive disks of gas and dust that are similar to protoplanetary disks around young stars. We assembled a catalog of all known Galactic post-AGB binaries with disks. We explore the correlations between the different observables with the aim of learning more about potential disk-binary interactions. We compiled spectral energy distributions of 85 Galactic post-AGB binary systems. We built a color-color diagram to differentiate between the different disk morphologies traced by the infrared excess. We categorized the different disk types and searched for correlations with other observational characteristics of these systems. Between 8 and 12that is, disks having no or low near-infrared excess. We find a strong link between these transition disks and the depletion of refractory elements on the surface of the post-AGB star. We interpret this link as evidence of a mechanism that stimulates the dust and gas separation within the disk and that also produces the transition disk structure. We propose that such a mechanism is likely to be due to a giant planet carving a hole in the disk, effectively trapping the dust in the outer disk parts. We propose disk evolutionary scenarios, depending on the presence of such a giant planet in the disk. We advocate that giant planets can successfully explain the link between the transition disks and the observed depletion of refractory materials. If the planetary scenario is confirmed, disks around post-AGB binaries could be a unique laboratory for testing planet-disk interactions and their influence on the late evolution of binary stars. The question of whether such planets are first- or second-generation bodies remains to be considered. We argue that these disks are ideal for studying planet formation in unprecedented parameter space.

15. Ammonia mapping observations toward the Galactic massive star-forming region Sh 2-255 and Sh 2-257

Mikito Kohno, Toshihiro Omodaka, Toshihiro Handa, James O. Chibueze, Takumi Nagayama, Ross A. Burns, Takeru Murase, Ren Matsusaka, Makoto Nakano, Kazuyoshi Sunada, Rin I. Yamada, John H. Bieging ★ We performed NH_3 $(J, K) = (1, 1), (2, 2)$, and $(3, 3)$ mapping observations toward the Galactic massive star-forming region Sh 2-255 and Sh 2-257 using the Nobeyama 45-m telescope as a part of the KAGONMA (KAgoshima Galactic Object survey with the Nobeyama 45-metre telescope by Mapping in Ammonia lines) project. NH_3 (1,1) has an intensity peak at the cluster S255 N, is distributed over 3 pc $\times$ 2 pc and is located between two HII regions. The kinetic temperature derived from the $NH_3(2, 2)/(1, 1)$ ratio was $\sim$ 35 K near the massive cluster S255 IR. These clusters also show emission with a large line width of $\sim$ 3-4 km s^{-1}. Based on the reported data we suggest that NH_3 gas in these regions is affected by stellar feedback from embedded YSO clusters in S255 IR and S255 N. We also detected NH_3 (1,1) emission in a region west of the main gas clump at the location of a concentration of Class II YSOs adjacent to the HII regions Sh 2-254. The presence of Class II YSOs implies $\sim$ 2 Myr of star formation, younger than Sh 2-254 ($\sim$ 5 Myr), thus we suggest that star formation in the western region could be influenced by the older HII region Sh 2-254.

16. Dynamics of magnetic flux tubes in accretion disks of Herbig Ae/Be stars

Sergey A. Khaibrakhmanov, Alexander E. Dudorov ★ The dynamics of magnetic flux tubes (MFTs) in the accretion disk of typical Herbig Ae/Be star with fossil large-scale magnetic field is modeled taking into account the buoyant and drag forces, radiative heat exchange with the surrounding gas, and the magnetic field of the disk. The structure of the disk is simulated using our magnetohydrodynamic (MHD) model, taking into account the heating of the surface layers of the disk with the stellar radiation. The simulations show that MFTs periodically rise from the innermost region of the disk with speeds up to $10 - 12$ km s^{-1}. MFTs experience decaying magnetic oscillations under the action of the external magnetic field near the disk's surface. The oscillation period increases with distance from the star and initial plasma beta of the MFT, ranging from several hours at $r = 0.012$ au up to several months at $r = 1$ au. The oscillations are characterized by pulsations of the MFT's characteristics including its temperature. We argue that the oscillations can produce observed IR-variability of Herbig Ae/Be stars, which would be more intense than in the case of T Tauri stars, since the disks of Herbig Ae/Be stars are hotter, denser and have stronger magnetic field.

17. Breaking Orion's Veil bubble with fossil outflows

U Kavak, J. R. Goicoechea, C. H. M. Pabst, J. Bally, F. F. S. van der Tak, A. G. G. M. Tielens ★ The role of feedback in the self-regulation of star formation is a fundamental question in astrophysics. The Orion Nebula is the nearest site of ongoing and recent massive star formation. It is a unique laboratory for the study of stellar feedback. Recent SOFIA [CII] 158 μm observations revealed an expanding bubble, the Veil shell, being powered by stellar winds and ionization feedback. We have identified a protrusion-like substructure in the Northwest portion of the Orion Veil Shell that may indicate additional feedback mechanisms that are highly directional. Our goal is to investigate the origin of the protrusion by quantifying its possible driving mechanisms. We use the [CII] 158 μm map of the Orion Nebula obtained with the upGREAT instrument onboard SOFIA. The spectral and spatial resolution of the observations are 0.3 km/s and 16 arcsec, respectively. We consider three possible origins for this protrusion: Fossil outflow cavities created by jets/outflows during the protostellar accretion phase, pre-existing clumpiness in the OMC-1 core, and the stellar wind during the main sequence phase. Based on the energetics and the morphology, we conclude that the northwestern part of the pre-existing cloud was locally perturbed by outflows ejected from massive protostars in the Trapezium cluster. This suggests that the protrusion of the Veil is the result of mechanical rather than radiative feedback. Furthermore, we argue that the location of the protrusion is a suitable place to break the Orion Veil owing to the photo-ablation from the walls of the protrusion. We conclude that the outflows of massive protostars can influence the morphology of the future HII,region and even cause breakages in the ionization front. Specifically, the interaction of stellar winds of main-sequence stars with the molecular core pre-processed by the protostellar jet is important.

18. Anisotropic Infall and Substructure formation in Embedded Disks

Aleksandra Kuznetsova, Jaehan Bae, Lee Hartmann, Mordecai-Mark Mac Low ★ The filamentary nature of accretion streams found around embedded sources suggest that protostellar disks experience heterogenous infall from the star-forming environment, consistent with the accretion behavior onto star-forming cores in top-down star-cluster formation simulations. This may produce disk substructures in the form of rings, gaps, and spirals continuing to be identified by high-resolution imaging surveys in both embedded Class 0/I and later Class II sources. We present a parameter study of anisotropic infall, informed by the properties of accretion flows onto protostellar cores in numerical simulations, and varying the relative specific angular momentum of incoming flows as well as their flow geometry. Our results show that anisotropic infall perturbs the disk and readily launches the Rossby wave instability (RWI). It forms vortices at the inner and outer edge of the infall zone where material is deposited. These vortices drive spiral waves and angular momentum transport, with some models able to drive stresses corresponding to a viscosity parameter on the order of $\alpha \sim 10^{-2}$. The resulting azimuthal shear forms robust pressure

bumps that act as barriers to radial drift of dust grains, as demonstrated by post-processing calculations of drift-dominated dust evolution. We discuss how a self-consistent model of anisotropic infall can account for the formation of millimeter rings in the outer disk as well as producing compact dust disks, consistent with observations of embedded sources.

19. Molecular Clouds Associated with H II regions and Candidates within l = 106.65° to 109.50° and b = −1.85° to 0.95°

Chun-Xue Liinst1, 2, Hong-Chi Wanginst1, 2, Yue-Hui Mainst1, Miao-Miao Zhangınst1, Chong Li ınst3, 4, Yu-Qing Zhengınst1 ★ We present a large-scale simultaneous survey of the CO isotopologues (^{12}CO, ^{13}CO, and C^{18}O) J = 1 − 0 line emission toward the Galactic plane region of l = 106.65° to 109.50° and b = −1.85° to 0.95° using the Purple Mountain Observatory 13.7 m millimeter-wavelength telescope. Except for the molecular gas in the solar neighborhood, the emission from the molecular gas in this region is concentrated in the velocity range of [−60, −35] km s^{-1}. The gas in the region can be divided into four clouds, with mass in the range of $\sim 10^3$ to 10^4 $M_\odot$. We have identified 25 filaments based on the ^{13}CO data. The median excitation temperature, length, line mass, line width, and virial parameter of the filaments are 10.89 K, 8.49 pc, 146.11 $M_\odot$ pc^{-1}, 1.01 km s^{-1}, and 3.14, respectively. Among these filaments, eight have virial parameters of less than 2, suggesting that they are gravitationally bound and can lead to star formation. Nineteen H II regions or candidates have previously been found in the region and we investigate the relationships between these H II regions/candidates and surrounding molecular clouds in detail. Using morphology similarity and radial velocity consistency between H II regions/candidates and molecular clouds as evidence for association, and raised temperature and velocity broadening as signatures of interaction, we propose that 12 H II regions/candidates are associated with their surrounding molecular clouds. In the case of the H II region of S142, the energy of the H II region is sufficient to maintain the turbulence in the surrounding molecular gas.

20. Testing Models of Triggered Star Formation with Young Stellar Objects in Cepheus OB4

Abby Mintz, Joseph L. Hora, Elaine Winston ★ OB associations are home to newly formed massive stars, whose turbulent winds and ionizing flux create H II regions rich with star formation. Studying the distribution and abundance of young stellar objects (YSOs) in these ionized bubbles can provide essential insight into the physical processes that shape their formation, allowing us to test competing models of star formation. In this work, we examined one such OB association, Cepheus OB4 (Cep OB4) - a well-suited region for studying YSOs due to its Galactic location, proximity, and geometry. We created a photometric catalog from Spitzer/IRAC mosaics in bands 1 (3.6 μm) and 2 (4.5 μm). We supplemented the catalog with photometry from WISE, 2MASS, IRAC bands 3 (5.8 μm) and 4 (8.0 μm), MIPS 24 μm, and MMIRS near IR data. We used color-color selections to identify 821 YSOs, which we classified using the IR slope of the YSOs' spectral energy distributions (SEDs), finding 67 Class I, 103 flat spectrum, 569 Class II, and 82 Class III YSOs. We conducted a clustering analysis of the Cep OB4 YSOs and fit their SEDs. We found many young Class I objects distributed in the surrounding shell and pillars as well as a relative age gradient of unclustered sources, with YSOs generally decreasing in age with distance from the central cluster. Both of these results indicate that the expansion of the H II region may have triggered star formation in Cep OB4.

21. Star Formation Triggered by the expanding bubble S111

Bhaswati Mookerjea ★ This paper investigates the impact of radiative and mechanical feedback from O-type stars on their parent molecular clouds and the triggering of formation of future generation of stars. We study the infrared bubble S111 created by the embedded massive stellar cluster G316.80-0.05. A significant fraction of gas in shells created due to the compression of the ambient medium by expanding bubbles is photodissociated by the stellar radiation. The kinematics of the shells are thus best studied using spectroscopic observations of singly ionized carbon, the most dominant species. We have used the velocity-resolved maps of the $^2P_{3/2} \rightarrow ^2 P_{1/2}$ transition of [C II] at 158 micron, the J=2-1 transition of 13CO and C18O, and the J=1-0 transition of HCO^+ to study the rim of the bubble S111 that partly coincides with the southern part of the infrared dark ridge G316.75. The [C II] spectra conclusively show evidence of a shell expanding with a moderate velocity of 7 km/s, which amounts to a kinetic energy that is 0.5-40 times the thermal energy of the H II region. The pressure causing the expansion of the H II region arises mainly from the hydrogen ionization and the dust-processed radiation. Among the far-infrared sources located in the compressed shells, we find the core G316.7799-0.0942 to show broad spectral features consistent with outflow activity and conclude that it is a site of active star formation. Based on the age of the H II region we conclude that this expanding H II region is responsible for the triggering of the current star formation activity in the region.

22. The width of Herschel filaments varies with distance

G. V. Panopoulou, S. E. Clark, A. Hacar, F. Heitsch, J. Kainulainen, E. Ntormousi, D. Seifried, R. J. Smith

★ Context: Filamentary structures in nearby molecular clouds have been found to exhibit a characteristic width of 0.1 pc, as observed in dust emission. Understanding the origin of this universal width has become a topic of central importance in the study of molecular cloud structure and the early stages of star formation. Aims: We investigate how the recovered widths of filaments depend on the distance from the observer, by using previously published results from the Herschel Gould Belt Survey. Methods: We obtained updated estimates on the distances to nearby molecular clouds observed with Herschel by using recent results based on 3D dust extinction mapping and Gaia. We examined the widths of filaments from individual clouds separately, as opposed to treating them as a single population. We used these per-cloud filament widths to search for signs of variation amongst the clouds of the previously published study. Results: We find a significant dependence of the mean per-cloud filament width with distance. The distribution of mean filament widths for nearby clouds is incompatible with that of farther away clouds. The mean per-cloud widths scale with distance approximately as 4–5 times the beam size. We examine the effects of resolution by performing a convergence study of a filament profile in the Herschel image of the Taurus Molecular Cloud. We find that resolution can severely affect the shapes of radial profiles over the observed range of distances. Conclusions: We conclude that the data are inconsistent with 0.1 pc being the universal characteristic width of filaments.

23. How D-type HII region expansion depends on numerical resolution

J. M. Pittard, M. M. Kupilas, C. J. Wareing ★ We investigate the resolution dependence of HII regions expanding past their Strömgren spheres. We find that their structure and size, and the radial momentum that they attain at a given time, is in good agreement with analytical expectations if the Strömgren radius is resolved with $dr \leq 0.3\,R_{\rm st}$. If this is not satisfied, the radial momentum may be over- or under-estimated by factors up to 10 or more. Our work has significance for the amount of radial momentum that a HII region can impart to the ambient medium in numerical simulations, and thus on the relative importance of ionizing feedback from massive stars.

24. Warping Away Gravitational Instabilities in Protoplanetary Discs

Sahl Rowther, Rebecca Nealon, Farzana Meru ★ We perform 3D SPH simulations of warped, non-coplanar gravitationally unstable discs to show that as the warp propagates through the self-gravitating disc, it heats up the disc rendering it gravitationally stable. Thus losing their spiral structure and appearing completely axisymmetric. In their youth, protoplanetary discs are expected to be massive and self-gravitating, which results in non-axisymmetric spiral structures. However recent observations of young protoplanetary discs with ALMA have revealed that discs with large-scale spiral structure are rarely observed in the midplane. Instead, axisymmetric discs with some also having ring & gap structures are more commonly observed. Our work invloving warps, non-coplanar disc structures that are expected to commonly occur in young discs, potentially resolves this discrepancy between observations and theoretical predictions. We demonstrate that they are able to suppress the large-scale spiral structure of self-gravitating protoplanetary discs.

25. First CH_3D detection in Class 0/I proto-brown dwarfs: constraints on CH_4 abundances

B. Riaz, W. -F. Thi ★ We report the first detection in the $J_K = 1_0$ - 0_0 rotational transition line of CH_3D towards three Class 0/I proto-brown dwarfs (proto-BDs) from IRAM 30 m observations. Assuming a rotational temperature of 25 K, the CH_3D abundances (relative to H_2) are in the range of (2.3–14.5) $\times$ 10^{-7}. The CH_4 abundances derived from the CH_3D abundances and assuming the DCO^+/HCO^+ ratios are in the range of (0.05–4.8) $\times 10^{-5}$. The gas-phase formation of CH_3D via CH_2D^+ is enhanced at high densities of 10^8–10^{10} cm^{-3} and our observations are likely probing the innermost dense and warm regions in proto-BDs. Thermal and/or non-thermal desorption can return the CH_3D and CH_4 molecules formed at an early stage on grain surfaces to the gas-phase. The gas phase abundances are indicative of warm carbon-chain chemistry in proto-BDs where carbon-chain molecules are synthesized in a lukewarm (∼20-30 K) region close to the central source.

26. Deuterium chemistry and D/H ratios in Class 0/I proto-brown dwarfs

B. Riaz, W. -F. Thi ★ We have conducted the first extensive observational survey of several deuterated species in 16 Class 0/I proto-brown dwarfs (proto-BDs) and 4 Class Flat/Class II brown dwarfs. Observations were obtained with the IRAM 30m telescope in the DCO^+ (3-2), DCN (3-2), DNC (3-2), and N_2D^+ (3-2) lines. The $DCO^+/H^{13}CO^+$, $DCN/H^{13}CN$, and $DNC/HN^{13}C$ ratios are comparatively higher and show a narrower range than the DCO^+/HCO^+, DCN/HCN, and DNC/HNC ratios, respectively. The mean D/H ratios for the proto-BDs derived from these molecules are in the range of ∼0.02-3. Both low-temperature gas-phase ion-molecule deuteron transfer and grain surface reactions are required to explain the enhanced deuterium fractionation. The very dense and cold (n_{H_2} $\geq 10^6$ cm^{-3}, T $\leq$10 K) interior of the proto-BDs provide the suitable conditions for efficient deuterium fractionation in these cores. There is no correlation between the D/H ratios and the CO depletion factor, with the exception of the DCN/HCN ratios that show a strong anti-correlation possibly due to the difference in the peak emitting regions of the DCN and HCN molecules. Over a wide range in the bolometric luminosities spanning

$\sim$0.002–40 $L_\odot$, we find a trend of higher DCO^+/HCO^+ (r = -0.7) and DCN/HCN (r = -0.6) ratios, nearly constant DNC/HNC (r = -0.4) and $DNC/HN^{13}C$ (r = -0.1) ratios, lower N_2D^+/N_2H^+ ratios (r = 0.6) in the proto-BDs compared to protostars. Only one Class II brown dwarf shows emission in the DCO^+ (3-2) line. No correlation is seen between the D/H ratios and the evolutionary stage.

27. Connecting Galactic and extragalactic outflows: From the Cygnus-X cluster to active galaxies

I. M. Skretas, L. E. Kristensen ★ Molecular outflows are often detected originating from both protostellar and extragalactic sources. Studies of low-mass, isolated high-mass, and extragalactic sources reveal scaling relations connecting the force carried by an outflow and the properties of the source that drives it. The aim of this work is to examine the effects of clustered star formation on the protostellar outflows and their scaling relations and to explore the possibility that outflows varying greatly scale and energetics are consistent with being launched by the same physical processes. High-angular resolution CO J = 3-2 observations were used of ten high-mass protostars in the Cygnus-X molecular cloud, obtained at the SMA as part of the PILS-Cygnus survey. From these data, the outflow force was measured. In addition, an extended sample of protostellar and extragalactic outflow-force measurements was assembled from existing literature to allow for a direct comparison of the scaling relations of the two types of outflows. Molecular outflows were detected originating from all ten sources of the PILS-Cygnus survey, and their outflow forces are found in close agreement with measurements from the literature. The comparison of the protostellar and extragalactic sources reveals, with 95% confidence, that Class 0 protostars and extragalactic sources follow the same outflow force–bolometric luminosity correlation. The close agreement between the Cygnus-X sources and sources of similar envelope mass and bolometric luminosity suggests that clustered star formation has no significant effect on protostellar outflows. We find a strong indication that protostellar and extragalactic outflows are consistent with having a similar launch mechanism. The existence of such a mechanism would enable the development of a single universal outflow launch model, although more observations are required in order to verify this connection.

28. ALMA High-resolution Multiband Analysis for the Protoplanetary Disk around TW Hya

Takashi Tsukagoshi, Hideko Nomura, Takayuki Muto, Ryohei Kawabe, Kazuhiro D. Kanagawa, Satoshi Okuzumi, Shigeru Ida, Catherine Walsh, Tom J. Millar, Sanemichi Z. Takahashi, Jun Hashimoto, Taichi Uyama, Motohide Tamura ★ We present a high-resolution (2.5 au) multiband analysis of the protoplanetary disk around TW Hya using ALMA long baseline data at Bands 3, 4, 6, and 7. We aim to reconstruct a high-sensitivity millimeter continuum image and revisit the spectral index distribution. The imaging is performed by combining new ALMA data at Bands 4 and 6 with available archive data. Two methods are employed to reconstruct the images; multi-frequency synthesis (MFS) and the fiducial image-oriented method, where each band is imaged separately and the frequency dependence is fitted pixel by pixel. We find that the MFS imaging with the second order of Taylor expansion can reproduce the frequency dependence of the continuum emission between Bands 3 and 7 in a manner consistent with previous studies and is a reasonable method to reconstruct the spectral index map. The image-oriented method provides a spectral index map consistent with the MFS imaging, but with a two times lower resolution. Mock observations of an intensity model were conducted to validate the images from the two methods. We find that the MFS imaging provides a high-resolution spectral index distribution with an uncertainty of < 10 %. Using the submillimeter spectrum reproduced from our MFS images, we directly calculated the optical depth, power-law index of the dust opacity coefficient (β), and dust temperature. The derived parameters are consistent with previous works, and the enhancement of β within the intensity gaps is also confirmed, supporting a deficit of millimeter-sized grains within the gaps.

29. A 16 au Binary in the Class 0 Protostar L1157 MMS

John J. Tobin, Erin G. Cox, Leslie W. Looney ★ We present VLA observations toward the Class 0 protostar L1157 MMS at 6.8 mm and 9 mm with a resolution of 0.04" (14 au). We detect two sources within L1157 MMS and interpret these sources as a binary protostar with a separation of 16 au. The material directly surrounding the binary system within the inner 50 au radius of the system has an estimated mass of 0.11 $M_\odot$, calculated from the observed dust emission. We interpret the observed binary system in the context of previous observations of its flattened envelope structure, low rates of envelope rotation from 5000 to 200 au scales, and an ordered, poloidal magnetic field aligned with the outflow. Thus, L1157 MMS is a prototype system for magnetically-regulated collapse and the presence of a compact binary within L1157 MMS demonstrates that multiple star formation can still occur within envelopes that likely have dynamically important magnetic fields.

30. ALMA observations of the Extended Green Object G19.01−0.03: I. A Keplerian disc in a massive protostellar system

Gwenllian M. Williams, Claudia J. Cyganowski, Crystal L. Brogan, Todd R. Hunter, John D. Ilee, Pooneh Nazari, J. M. Diederik Kruijssen, Rowan J. Smith, Ian A. Bonnell ★ Using the Atacama Large Millimetre/submillimeter Array (ALMA) and the Karl G. Jansky Very Large Array (VLA), we observed the Extended Green Object (EGO) G19.01−0.03 with sub-arcsecond resolution from 1.05 mm to 5.01 cm wavelengths. Our $\sim 0.4''$ ~ 1600 AU angular resolution ALMA observations reveal a velocity gradient across the millimetre core MM1, oriented perpendicular to the previously known bipolar molecular outflow, that is consistently traced by 20 lines of 8 molecular species with a range of excitation temperatures, including complex organic molecules (COMs). Kinematic modelling shows the data are well described by models that include a disc in Keplerian rotation and infall, with an enclosed mass of $40-70 M_\odot$ (within a 2000 AU outer radius) for a disc inclination angle of $i = 40°$, of which $5.4-7.2 M_\odot$ is attributed to the disc. Our new VLA observations show that the 6.7 GHz Class II methanol masers associated with MM1 form a partial ellipse, consistent with an inclined ring, with a velocity gradient consistent with that of the thermal gas. The disc-to-star mass ratio suggests the disc is likely to be unstable and may be fragmenting into as-yet-undetected low mass stellar companions. Modelling the centimetre–millimetre spectral energy distribution of MM1 shows the ALMA 1.05 mm continuum emission is dominated by dust, whilst a free-free component, interpreted as a hypercompact HII region, is required to explain the VLA ∼5 cm emission. The high enclosed mass derived for a source with a moderate bolometric luminosity ($\sim 10^4 L_\odot$) suggests that the MM1 disc may feed an unresolved high-mass binary system.

31. Magnetic Spirals in Accretion Flows Originated from Misaligned Magnetic Field

Weixiao Wang, Miikka S. Väisälä, Hsien Shang, Ruben Krasnopolsky, Zhi-Yun Li, Ka Ho Lam, Feng Yuan ★ Misalignment between rotation and magnetic field has been suggested to be one type of physical mechanisms which can easen the effects of magnetic braking during collapse of cloud cores leading to formation of protostellar disks. However, its essential factors are poorly understood. Therefore, we perform a more detailed analysis of the physics involved. We analyze existing simulation data to measure the system torques, mass accretion rates and Toomre Q parameters. We also examine the presence of shocks in the system. While advective torques are generally the strongest, we find that magnetic and gravitational torques can play substantial roles in how angular momentum is transferred during the disk formation process. Magnetic torques can shape the accretion flows, creating two-armed magnetized inflow spirals aligned with the magnetic field. We find evidence of an accretion shock that is aligned according to the spiral structure of the system. Inclusion of ambipolar diffusion as explored in this work has shown a slight influence in the small scale structures but not in the main morphology. We discuss potential candidate systems where some of these phenomena could be present.

32. Dissecting the different components of the modest accretion bursts of the very young protostar HOPS 373

Sung-Yong Yoon, Gregory J. Herczeg, Jeong-Eun Lee, Ho-Gyu Lee, Doug Johnstone, Watson Varricatt, John J. Tobin, Carlos Contreras Peña, Steve Mairs, Klaus Hodapp, P. Manoj, Mayra Osorio, S. Thomas Megeath, the JCMT Transient Team ★ Observed changes in protostellar brightness can be complicated to interpret. In our JCMT Transient monitoring survey, we discovered that a young binary protostar, HOPS 373, is undergoing a modest 30% brightness increase at 850 μm, caused by a factor of 1.8−3.3 enhancement in the accretion rate. The initial burst occurred over a few months, with a sharp rise and then shallower decay. A second rise occurred soon after the decay, and the source is still bright one year later. The mid-IR emission, the small-scale CO outflow mapped with ALMA, and the location of variable maser emission indicate that the variability is associated with the SW component. The near-infrared and NEOWISE $W1$ and $W2$ emission is located along the blueshifted CO outflow, spatially offset by $\sim$ 3 to $4''$ from the SW component. The K-band emission imaged by UKIRT shows a compact H_2 emission source at the edge of the outflow, with a tail tracing the outflow back to the source. The $W1$ emission, likely dominated by scattered light, brightens by 0.7 mag, consistent with expectations based on the sub-mm lightcurve. The signal of continuum variability in K-band and $W2$ is masked by stable H_2 emission, as seen in our Gemini/GNIRS spectrum, and perhaps by CO emission. These differences in emission sources complicate infrared searches for variability of the youngest protostars.

33. A large population study of protoplanetary disks: Explaining the millimeter size-luminosity relation with or without sub-structure

Apostolos Zormpas, Tilman Birnstiel, Giovanni P. Rosotti, Sean M. Andrews ★ Recent sub-arcsecond resolution surveys of the dust continuum emission from nearby protoplanetary disks showed a strong correlation between the sizes and luminosities of the disks. We aim to explain the origin of the (sub-)millimeter size-luminosity relation (SLR) between the 68% effective radius (r_{eff}) of disks with their continuum luminosity (L_{mm}), with models of gas and dust evolution in a simple viscous accretion disk and radiative transfer calculations. We use a large grid of models (10^5 simulations) with and without planetary gaps, varying the initial conditions of the key parameters. We calculate the disk continuum emission and the effective radius for all models as a function of time. By selecting those simulations that continuously follow the SLR, we can derive constraints

on the input parameters of the models. We confirm previous results that models of smooth disks in the radial drift regime are compatible with the observed SLR ($L_{mm} \propto r_{eff}^2$) but only smooth disks cannot be the reality. We show that the SLR is more widely populated if planets are present. However they tend to follow a different relation than smooth disks, potentially implying that a mixture of smooth and sub-structured disks are present in the observed sample. We derive a SLR ($L_{mm} \propto r_{eff}^{5/4}$) for disks with strong sub-structure. To be compatible with the SLR, models need to have an initially high disk mass ($\geq 2.5 \cdot 10^{-2} M_\star$) and low turbulence-parameter α values ($\leq 10^{-3}$). Furthermore, we find that the grain composition and porosity drastically affects the evolution of disks on the size-luminosity diagram where relatively compact grains that include amorphous carbon are favoured. Moreover, a uniformly optically thick disk with high albedo (0.9) that follows the SLR cannot be formed from an evolutionary procedure.

34. Star formation near the Sun is driven by expansion of the Local Bubble

Catherine Zucker, Alyssa A. Goodman, João Alves, Shmuel Bialy, Michael Foley, Joshua S. Speagle, Josefa Großschedl, Douglas P. Finkbeiner, Andreas Burkert, Diana Khimey, Cameren Swiggum ★ For decades we have known that the Sun lies within the Local Bubble, a cavity of low-density, high-temperature plasma surrounded by a shell of cold, neutral gas and dust. However, the precise shape and extent of this shell, the impetus and timescale for its formation, and its relationship to nearby star formation have remained uncertain, largely due to low-resolution models of the local interstellar medium. Leveraging new spatial and dynamical constraints from the Gaia space mission, here we report an analysis of the 3D positions, shapes, and motions of dense gas and young stars within 200 pc of the Sun. We find that nearly all the star-forming complexes in the solar vicinity lie on the surface of the Local Bubble and that their young stars show outward expansion mainly perpendicular to the bubble's surface. Tracebacks of these young stars' motions support a scenario where the origin of the Local Bubble was a burst of stellar birth and then death (supernovae) taking place near the bubble's center beginning 14 Myr ago. The expansion of the Local Bubble created by the supernovae swept up the ambient interstellar medium into an extended shell that has now fragmented and collapsed into the most prominent nearby molecular clouds, in turn providing robust observational support for the theory of supernova-driven star formation.